

Spatially Resolved Inter-electron Interaction of Autoionising States*

J. G. Story,^A D. I. Duncan^B and T. F. Gallagher^B

^A Department of Physics, University of Missouri-Rolla, Rolla, MO 65401, USA.

^B Department of Physics, University of Virginia, Charlottesville, VA 22901, USA.

Abstract

We have observed transitions to autoionising states in Mg using two short optical pulses. Mg atoms are initially prepared in a high lying Rydberg wave packet with the first picosecond (ps) laser. A second ps laser is then used to excite the inner electron, producing an autoionising state. The dependence of the transition probability on the delay between the two lasers shows that when the second laser is tuned away from the ionic resonance, the inner electron can make a transition only when the Rydberg wave packet is near the core.

1. Introduction

Atoms in which two electrons are in excited states provide an interesting challenge for both experimental and theoretical study. The interaction between the two excited electrons, as would be expected, plays a critical role in the structure of doubly excited atoms as well as the evolution of nonstationary states of these atoms. Generally a given doubly excited state cannot easily be identified in terms of two independent electron configurations. For doubly excited states with total energy above the first ionisation limit of the atom, these states decay primarily through autoionisation. Autoionisation occurs when the two electrons exchange energy, with one electron gaining sufficient energy to leave the atom producing a free electron and ion. Spectroscopic study of the autoionising energy region of alkaline earth atoms reveals a great deal of atomic structure corresponding to doubly excited states. The analysis of this structure is complicated due to the many possible two electron configurations which make up these states. In the case of autoionising Rydberg states, however, a single two electron configuration often describes the states reasonably well to lowest order. An autoionising Rydberg state is comprised of one electron in a highly excited Rydberg state and the other electron in a lower lying excited state. The Rydberg electron wave function has a large spatial extent, whereas the lower lying electron is confined near the ionic core of the atom. Because of the small overlap between the two electrons, the interaction between them is small

* Refereed paper based on a contribution to the Advanced Workshop on Atomic and Molecular Physics, held at the Australian National University, Canberra, in February 1995.

and the autoionising states are reasonably well described by two independent electron states such as the $3pnd$ state of Mg. In this states the nd electron is a Rydberg electron with principal quantum number n and the $3p$ electron represents an excited ionic state. The coupling between this configuration and other two electron configurations, including continuum configurations, can be calculated using multichannel quantum defect theory (MQDT).

The excitation of these autoionising Rydberg states can be performed using an efficient multi-step excitation method which provides a great deal of control over the choice of autoionising states excited. This method, known as the isolated core excitation (ICE) method (Cooke *et al.* 1978) has been used to gather a wealth of spectral information about doubly excited autoionising states of alkaline earth atoms (Sandner 1987). The essence of the ICE method is easily understood using Mg as an example (Dai *et al.* 1990). Atoms are first excited to a bound Rydberg state, e.g. $3snd$ in Mg, then optically excited to the autoionising $3pnd$ state. The $3snd \rightarrow 3pnd$ transition is essentially the $Mg^+ 3s \rightarrow 3p$ transition with the outer nd electron remaining a spectator. The absorption has a maximum near the frequency of the $Mg^+ 3s \rightarrow 3p$ resonance line and to a first approximation, the position and width of the maximum give the energy and spectral width of the autoionising $3pnd$ state.

The above isolated resonance description accurately describes the spectrum for small detunings from the ionic line. It is not, however, useful for larger detunings. When the light is detuned from the ionic transition, the binding energy of the Rydberg electron must be altered by the amount of the detuning to conserve energy. When the detuning exceeds the energy interval ΔW_n between the Rydberg states, shakeup satellites corresponding to the excitation of the adjacent autoionising Rydberg states appear clearly in the spectrum (Tran *et al.* 1984; Bhatti and Cooke 1983). During the excitation of a satellite resonance the Rydberg electron must change its principal quantum number which suggests that there is interaction between the two electrons during the excitation process. Applying quantum defect theory (QDT) to the above notion of an ionic transition with a spectator electron has been successful in reproducing the entire ICE spectrum, including the shakeup satellites. In the QDT analysis, the Rydberg electron experiences a new ionic potential due to the excitation of the core. Since the initial and final potential is not the same, final Rydberg states with different values of n need not be orthogonal to the initial state. The lack of orthogonality allows n changing transitions of the Rydberg electron.

A point which is not transparent in the QDT description is that the Rydberg electron is located in different places for on- and off-resonant absorption. In on-resonant absorption the Rydberg electron does not change states during the excitation, so that it need not be present near the Mg^+ ionic core when the photon is absorbed. In fact, it is most likely to be near its outer turning point since that is where the electron spends most of its time during its orbit. In contrast, in off-resonant absorption the photon's energy is shared between the ion and the Rydberg electron, requiring that they be close together when the photon absorption occurs.

Here we report the results of an experimental test of the above notions using short pulse ICE of a bound wave packet. The utility of using short pulse ICE to probe the dynamics of autoionisation was first suggested by Wang and Cooke

(1991). They later demonstrated that with short pulse ICE it was possible to make a notch in a bound Rydberg state wave function, creating an anti-wave packet (Wang and Cooke 1992*a,b*). A related method of producing anti-wave packets has been reported by Noordam *et al.* (1992), and short pulse ionisation of the core but not the Rydberg electron has been reported by Jones and Bucksbaum (1991) and Stapelfeldt *et al.* (1991). Our experiment is done by using a ps laser to produce a localised radial wave packet of bound Mg $3snd$ states so that the nd electron oscillates between the core and its outer turning point (ten Wolde *et al.* 1988; Parker and Stroud 1986; Alber *et al.* 1986; Yeazell *et al.* 1990). With a second synchronised ps laser tuned on or off the $Mg^+ 3s \rightarrow 3p$ transition, we can drive the $3snd \rightarrow 3pn_d$ transition when the Rydberg electron is either near to or far from the ion core. The experiments show that on-resonant absorption occurs whether the Rydberg electron is far from or near to the core, but that off-resonant absorption occurs only when the Rydberg electron is near the core. We show that the observed dependence on the spatial position of the Rydberg electron can be derived from a generalisation of the QDT used to describe the ICE shakeup spectrum. Our theoretical approach is similar to the one developed by Wang and Cooke (1991, 1992*a*, 1992*b*) to describe short pulse ICE. A more general QDT description of wave packets in two electron systems has been given by Henle *et al.* (1987).

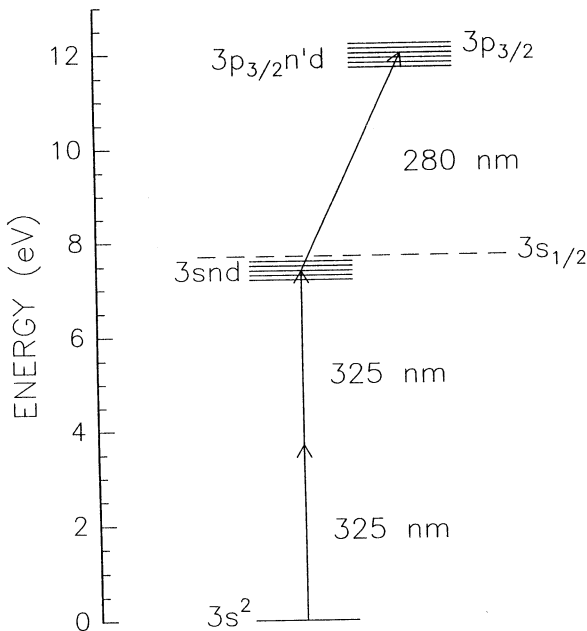


Fig. 1. The excitation path used in the experiment is shown. Two photons of doubled 650 nm light excite Mg to a $3snd \ ^1D_2$ Rydberg wave packet state, where n is the central state of the wave packet. One photon of the doubled 560 nm light then excites the $3s$ core electron, producing $3p_{3/2}n'd$ autoionising states, where n' is the central state of the final Rydberg wave packet.

2. Experiment

In the experiment an effusive Mg beam from a heated oven passed between a pair of plates 10 cm from the oven. Between the plates atoms were excited by two synchronised uv ps laser pulses as shown in Fig. 1. The first pulse, at 325 nm, drove the $3s^2 \rightarrow 3snd$ two photon transition creating a radial wave packet of $3snd$ states. The second laser pulse, at 280 nm, drove the $3snd \rightarrow 3p_{3/2}nd$ transition after a variable delay. Following the laser pulses, the ions from the decay of autoionising $3pnd$ states were detected by applying a 60 V cm^{-1} field pulse to the plates to drive the Mg^+ ions to a microchannel plate detector.

The synchronised ps uv pulses were produced as follows. A frequency doubled Coherent Antares mode locked Nd:YAG laser was used to pump two Coherent 700 mode locked tunable dye lasers. The first dye laser, tuned to 650 nm, had a temporal width of 3.2 ps (FWHM), and the second, tuned to 560 nm had a temporal width of 5.2 ps. Because the two lasers were pumped by the same source the timing jitter between the two pulses was less than 2 ps. The two dye laser beams were amplified in three stage dye amplifiers pumped by a Nd:YAG regenerative amplifier and then frequency doubled using KDP crystals. The delay between the two laser pulses was adjusted using a delay line in the 560 nm laser beam path which could be scanned continuously. The uv beams were focused when they crossed the Mg atomic beam inside the vacuum chamber. Data were taken by fixing the detuning of the second laser from the ion resonance and scanning the delay between the two lasers. Positive delay corresponds to the second laser pulse coming after the first.

Fig. 2 shows typical data obtained with this method. For these data the first laser was tuned to excite a wave packet centred at $n_0 = 54$ with a classical orbital period of 24 ps. The second laser was tuned approximately 15 cm^{-1} above the $\text{Mg}^+ 3s \rightarrow 3p_{3/2}$ transition. The large initial peak in the data is due to enhanced multiphoton ionisation of the ground state of Mg when the two lasers are temporarily overlapped. There are two additional peaks, at 25 and 50 ps, which correspond to the first and second returns of the Rydberg wave packet to the core. The third peak, the second return, is broadened by dispersion of the wave packet. Beyond the second return, the wave packet is sufficiently dispersed so that no additional structure can be observed. These data clearly show that the Rydberg electron must be near the core in order for the core electron to make an off-resonant transition.

Data were taken with the first laser tuned to different n states and, as expected, the signal oscillated with the orbital period of $2\pi n_0^3$. Fig. 3 shows data taken with $n = 54$ and 45. The width of the initial peaks for both data is the same, consistent with the length of the laser pulses. The resolution of the oscillations is poor in the case of the $n = 45$ data due to the width of the peaks, but oscillations can clearly be seen with a period of 14 ps which is approximately the classical oscillation time of the $n = 45$ wave packet.

Data were also taken for different detunings of the second laser from the ionic transition, and examples are shown in Fig. 4 along with calculated spectra. The laser detunings from resonance are accurate to 10 cm^{-1} . In Fig. 4a we show the ionisation signal for the core laser tuned to the $3s \rightarrow 3p_{3/2}$ ion resonance. As shown, the signal goes from zero for negative delay to a plateau for positive delay, and there are 20% oscillations due to the first and second returns of the Rydberg

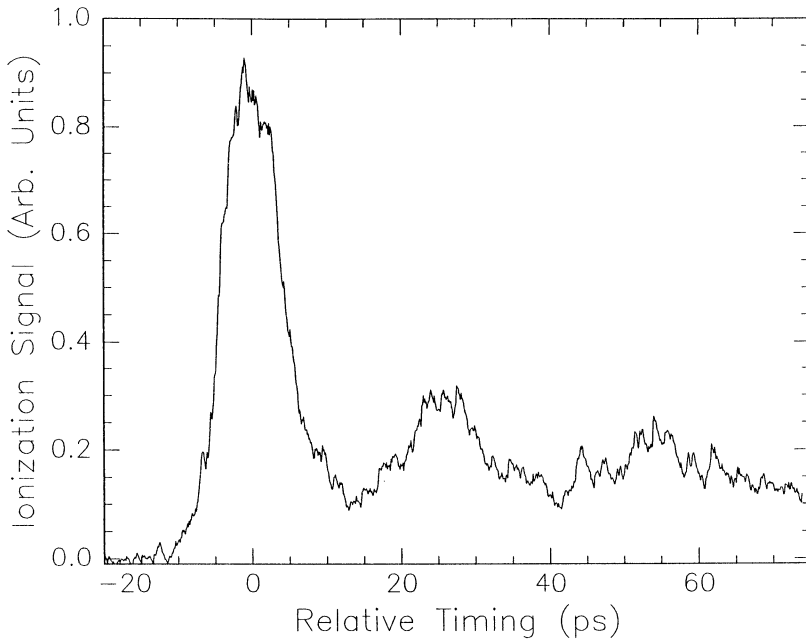


Fig. 2. A time resolved excitation spectrum is shown where the initial Rydberg state is centred around $n = 54$ and the core laser is tuned approximately 15 cm^{-1} to the blue of the ionic resonance. The time axis represents the relative timing between the Rydberg and core laser. Peaks are seen in the excitation spectra when the relative timing is equal to an integral number of classical orbital periods of the central Rydberg state of the wave packet. For $n = 54$ the classical orbital period is 24 ps.

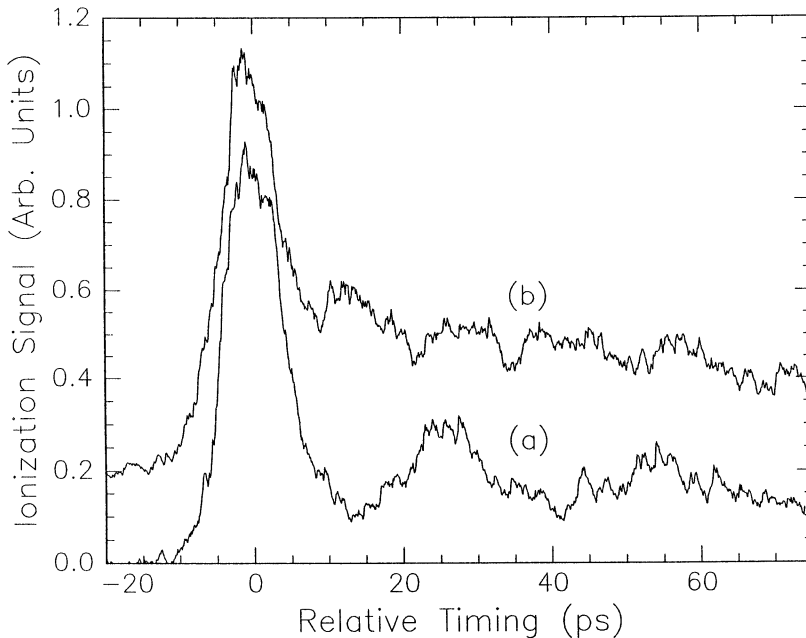


Fig. 3. Time resolved excitation spectra are shown for an initial Rydberg wave packet centred around (a) $n = 54$ and (b) $n = 45$, with a detuning of 15 cm^{-1} from the ionic transition. The oscillation periods correspond approximately to the classical orbit periods of 24 and 14 ps for the $n = 54$ and 45 states respectively. The $n = 45$ spectra is slightly offset in the vertical axis for clarity.

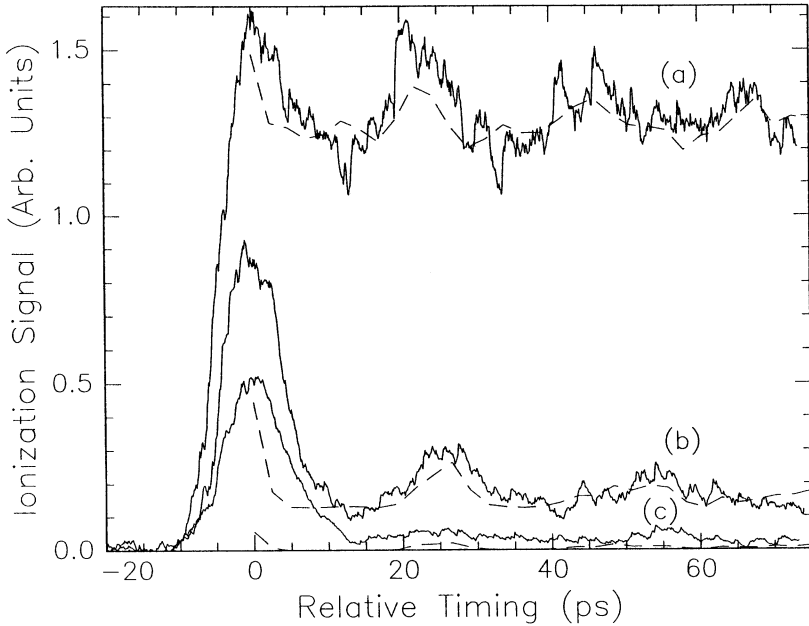


Fig. 4. Measured and calculated spectra are shown for several tunings of the core laser with the Rydberg laser tuned to $n = 54$. Near the ionic resonance, (a), a large baseline signal results from the resonant excitation of the core electron which is largely independent of the position of the Rydberg electron. Away from the ionic resonance, (b) and (c), the shakeup excitation exhibits a strong dependence on the Rydberg electron position.

electron to the core at the classical orbital period. In other words the atom has a high probability of making the $3snd \rightarrow 3p_{3/2}nd$ transition irrespective of the spatial position of Rydberg electron. As the detuning is increased to 15 cm^{-1} , in Fig. 4b, the signal for positive delays exhibits the same structure as shown in Fig. 2: a large peak at zero delay followed by two peaks due to the first and second returns of the wave packet to the core. Fig. 4c shows data taken with a detuning of 30 cm^{-1} . Except for the multiphoton peak at zero delay, the signal level has dropped considerably. However, the increases due to the first and second return of the wave packet are still discernable. These experimental data indicate that the Rydberg electron must be near the core for off-resonant excitation of the ionic transition.

3. Theory

It is instructive to consider a simple physical picture of the interaction between the two electrons during the excitation. The initial Rydberg state before the excitation of the core is bound to the ionic core by a net attractive potential due to the nucleus and inner electrons. When one of the inner electrons is excited the potential seen by the Rydberg electron is changed. This changing potential allows the energy of the Rydberg electron to change so that it can share the energy of the photon allowing an off-resonant ionic transition to occur. However, the spatial region over which the potential is changed is determined by the size of the excited ionic state. At large r the Rydberg electron sees only the Coulomb potential. If the Rydberg electron is localised at large r during the laser pulse

it sees no change in the potential and cannot change energy. In this case the off-resonant excitation of the ionic core cannot occur. On-resonant excitation, on the other hand, requires no change of energy of the Rydberg electron and is much less sensitive to the position of the Rydberg electron.

To show the connection between the time resolved spectra of Fig. 4 and the theory used to describe time independent ICE spectra, we briefly describe the generation of the synthetic spectra of Fig. 3. A bound Rydberg $3snd$ state has the energy $W_n = -\frac{1}{2}n^{*-2}$ relative to the Mg^+ $3s$ state, implicitly defining the effective quantum number n^* . Similarly, at an energy $W_\nu = -\frac{1}{2}\nu^{-2}$ relative to the Mg^+ $3p$ state, the $3pnd$ wavefunction has an effective quantum number ν . Unlike n^* , ν is continuous since the autoionising $3pnd$ states are coupled to the $3s\epsilon f$ continua. The ICE transition matrix element is easily given in terms of the effective quantum numbers n^* and ν as (Bhatti *et al.* 1981):

$$T_n(\nu) = A(\nu)\mu \left(\frac{\sin[\pi(n^* - \nu)]}{\pi(\frac{1}{2}n^{*2} - \frac{1}{2}\nu^2)} \right). \quad (1)$$

Here μ is the constant ionic dipole matrix element, and $A^2(\nu)$ is the density of the final autoionising states, which is peaked at the location of the Mg $3pnd$ states, at $\nu = n'$, the widths of the peaks giving the autoionisation rates. The bracketed term of (1) represents the overlap of the bound nd wavefunction with the autoionising νd wave function. Squaring (1) gives the frequency dependence of the ICE spectrum. For $|n^* - \nu| < 1$, the bracketed term is constant and the spectrum is determined entirely by $A^2(\nu)$, which depends on the energies and widths of the nd autoionising states. In our experiment the bound intermediate state is not a stationary state but a wave packet with a wave function given by

$$\psi_1(t) = \sum C_n \psi_n e^{-it/2n^{*2}}, \quad (2)$$

where C_n is the amplitude of the n th state which is determined by the tuning and spectral width of the first laser. If the central frequency of the first laser excites the state with principal quantum number n_0 and the bandwidth of the laser is Γ_1 , then C_n is given by

$$C_n = \exp[-(W_{n_0} - W_n)^2/\Gamma_1^2]. \quad (3)$$

To describe the excitation by the two short pulses, we combine the Rydberg wave packet of (2) with the transition matrix element of (1) for each final state energy or, equivalently, each value of ν . The transition probability to the final state energy W_ν from the ground state is given by

$$T_g(\nu) = \left| \sum C_n C_{n\nu} T_n(\nu) e^{-it/2n^{*2}} \right|^2, \quad (4)$$

where $C_{n\nu}$ reflects the number of bound states coupled to the final state energy W_ν due to the bandwidth of the second laser. For a Gaussian pulse, $C_{n\nu}$ is given by

$$C_{n\nu} = \exp[(W_\nu - W_n - \omega)^2/\Gamma_2^2], \quad (5)$$

where ω is the second photon's energy and Γ_2 is the bandwidth of the second laser pulse. Squaring (3) gives the ionisation signal for any value of final state energy W_ν , and integrating over ν we obtain an expression proportional to the observed ionisation signal S . Explicitly, we have

$$S = \int |T_g(\nu)|^2 d\nu. \quad (6)$$

The calculated curves shown by the dashed lines of Fig. 4 have been obtained using (6).

The one parameter which was adjusted to fit the data was the detuning from the ion resonance. In the calculations, the size of the resonant plateau for positive delays was rather sensitive to the detuning of the core laser from the ionic resonance. Since the tuning of the core laser was known only to within 10 cm^{-1} , we adjusted the detuning to best fit the data. The fit detunings were 8, 13 and 25 cm^{-1} , in reasonable agreement with the measured values of 0, 15 and 30 cm^{-1} . With this single adjustable parameter, the theoretical spectra show excellent agreement with the data for positive delays. The calculation does not agree with the measurement at zero delay, because it does not include multiphoton ionisation of the ground state due to the temporal overlap of the lasers.

4. Conclusion

These data clearly show that the Rydberg electron must be near the core to excite the inner electron away from the ionic resonance whereas, for core excitation near the ionic resonance, the position of the Rydberg electron is relatively unimportant and, in theory, should be far from the core. We note that the theory predicts that if the core laser is tuned on the ionic resonance there should be a decrease, not an increase, in the ionisation signal at the returns of the wave packet to the core due to broadening of the ionic transition beyond the laser linewidth. We have not yet observed this phenomenon, but the good agreement between theory and experiment leads us to conclude that the QDT model is valid for excitation by short pulses.

Acknowledgment

This work was supported by the US Department of Energy, Division of Chemical Sciences, Office of Basic Energy Sciences.

References

- Alber, G., Ritsch, H., and Zoller, P. (1986). *Phys. Rev. A* **56**, 1058.
 Bhatti, S. A., and Cooke, W. E. (1983). *Phys. Rev. A* **28**, 756.
 Bhatti, S. A., Cromer, C. L., and Cooke, W. E. (1981). *Phys. Rev. A* **24**, 161.
 Cooke, W. E., Gallagher, T. F., Edelstein, S. A., and Hill, R. M. (1978). *Phys. Rev. Lett.* **40**, 178.
 Dai, C. J., Schinn, G. W., and Gallagher, T. F. (1990). *Phys. Rev. A* **42**, 223.
 Henle, W. A., Ritsch, H., and Zoller, P. (1987). *Phys. Rev. A* **36**.
 Jones, R. R., and Bucksbaum, P. H. (1991). *Phys. Rev. Lett.* **67**, 3215.
 Noordham, L. D., Stapelfeldt, H., Duncan, D. I., and Gallagher, T. F. (1992). *Phys. Rev. Lett.* **68**, 1496.
 Parker, J., and Stroud, C. R. Jr (1986). *Phys. Rev. Lett.* **56**, 716.

- Sandner, W. (1987). *Comm. At. Mol. Phys.* **20**, 171.
- Staplefeldt, D. G., Papaioannou, D. G., Noordam, L. D., and Gallagher, T. F. (1991). *Phys. Rev. Lett.* **67**, 3223.
- ten Wolde, A., Noordam, L. D., Lagendijk, A., van Linden van den Heuvell, H. B. (1988). *Phys. Rev. Lett.* **61**, 2099.
- Tran, N. H., Pillet, P., Kachru, R., and Gallagher, T. F. (1984). *Phys. Rev. A* **29**, 2640.
- Wang, X., and Cooke, W. E. (1991). *Phys. Rev. Lett.* **67**, 976.
- Wang, X., and Cooke, W. E. (1992a). *Phys. Rev.* **46**, R2201.
- Wang, X., and Cooke, W. E. (1992b). *Phys. Rev.* **46**, 4347.
- Yeazell, J. A., Mallallieu, M., and Stroud, C. R. Jnr (1990). *Phys. Rev. Lett.* **64**, 2007.

Manuscript received 15 February, accepted 18 October 1995

